2016 IEEE/RSJ International Conference on Intelligent Robots and Systems (IROS)
Daejeon Convention Center
October 9-14, 2016, Daejeon, Korea

Elastic Energy Storage in Leaf Springs for a Lever-Arm Based Variable Stiffness Actuator

Eamon Barrett[1], Matteo Fumagalli[2], and Raffaella Carloni[1]

Abstract— **The increasing use of Variable Stiffness Actuators (VSAs) in robotic joints is helping robots to meet the demands of human-robot interaction, requiring high safety and adaptability. The key feature of a VSA is the ability to exploit internal elastic elements to obtain a variable output stiffness. These allow the joints to store mechanical energy supplied through interaction with the environment and make the system more robust, efficient, and safe. This paper discusses the design of leaf springs for a sub-class of VSAs that use variable lever arm ratios as means to change their output stiffness. Given the trade-off between compactness and the maximum energy storage capacity, the internal springs' dimensions and material choice are assessed through a theoretical analysis and practical experiments.**

I. INTRODUCTION

Equipping robotic joints with mechanically compliant elements has established itself as a means to meet the demands of robots intended for human-robot interaction. In future, robots will be expected to closely interact with humans and unknown environments. Therefore robots and their actuators need to be intrinsically safe, compact and light weight, and energy efficient, while still having a large energy capacity.

The compliant elements in the joints absorb impact forces, leading to increased safety for both the robot and its environment [1], while reducing the required control effort by embodying a desired behavior in the system's natural dynamics [2], store mechanical energy, increase energy efficiency [1], and increase the peak output power of an actuator [3].

Variable Stiffness Actuators (VSAs) are capable of changing their output stiffness, which makes them suited for a wide range of tasks and enables them to tune their natural dynamics. A large number of different VSAs have been presented in the recent years [4]. VSAs can be grouped by the way they achieve a variable output stiffness, namely by adjusting the spring preload [5], [6], adjusting the transmission between spring and load [7], [8], [9], or adjusting the physical properties of the spring.

Independent of their operating principle, however, all VSAs require internal springs to store mechanical energy during interaction. The design of which is a trade-off between the weight and size of these springs on the one hand, and their energy storage capacity on the other. Given the high requirements in terms of weight and compactness, as well as output loads and energy storage, the proper selection of the spring type, material, and dimensions, is of great importance for a large torque-deflection workspace.

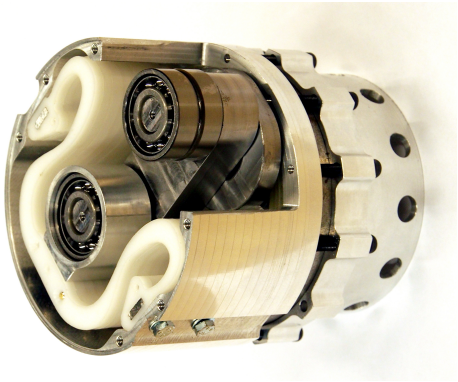

Fig. 1: Lever-arm based stiffness adjustment mechanism equipped with an Ω-shaped polymer (POM) leaf spring.

The contribution of this paper lies in the analysis of the effect that the selection and design of the internal springs has on the performance of lever-arm based VSAs, in particular on the energy storage capacity, which is limited by the compactness of the system. The working principle and requirements for lever-arm based VSAs are presented, along with a design methodology that maximizes the energy storage for such actuators. This methodology is based on an analysis of the relations between the spring parameters and validated by simulation and experimental results on the Stiffness Adjustment Mechanism (SAM) shown in Fig. 1.

This paper is organized as follows. Section II presents the lever-arm based SAM and derives requirements for the internal springs. Section III presents the analysis and design methodology for the springs. Section IV validates the design of these springs with experimental results. The results are discussed in Section V and, finally, concluding remarks are made in Section VI.

II. STIFFNESS ADJUSTMENT MECHANISM

VSAs that are based on a variable transmission, for instance achieved through variable lever arm ratios, can operate energy efficiently [10], i.e. they can change their output stiffness without changing the energy stored in the springs. This makes them well suited for a design approach, that aims at maximizing the energy a VSA can absorb from the environment.

This work has been funded by the European Commission's 7^{th} Framework Programme as part of the project SHERPA under grant no. 600958.

[1]E. Barrett and R. Carloni are with the Faculty of Electrical Engineering, Mathematics and Computer Science, CTIT Institute, University of Twente, The Netherlands. Email: {e.barrett,r.carloni}@utwente.nl.

[2]M. Fumagalli is with the Department of Mechanical and Manufacturing Engineering, Aalborg University, Denmark. Email: m_fumagalli@m-tech.aau.dk. (Research performed while M. Fumagalli was within the Faculty of Electrical Engineering, Mathematics and Computer Science, CTIT Institute, University of Twente, The Netherlands.)

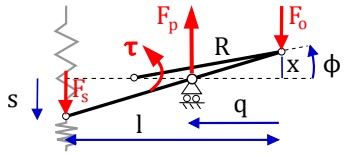

Fig. 2: Concept of a lever arm based SAM: the pivot position q determines the transmission between output x and spring deflection and s.

The working principle of a lever-arm-based SAM is presented in this section, and design requirements are derived from an analysis of its internal loads and the way the SAM stores energy in its internal springs.

A. Lever-arm based SAM

A lever-arm based SAM realizes a variable transmission between the output and the internal springs by changing the lever arm ratio between the two, which is best done by moving the pivot point along the lever [7]. The equations presented in this section use approximations for small output deflections, but still offer a good representation of the mechanism's properties and are a useful tool for analysis.

With reference to Fig. 2, a crank with length R transforms the linear force F_o and deflection x of the lever into the rotational torque τ and deflection ϕ. A deflection $x = \sin(\phi)R$ of the lever at the connection with the output causes an elongation s of the spring:

$$s = \frac{l-q}{q}\, x = \frac{l-q}{q}\, \sin(\phi)\, R \tag{1}$$

where l is the length of the lever, and q the position of the pivot point of the lever. Note that if more than one spring is connected to the lever, usually in an antagonistic setup, they can be considered as a single virtual spring.

The internal forces on the lever at the connection points with the springs, output, and pivot are

$$F_s = k_s \cdot s, \qquad F_o = \frac{l-q}{q} \cdot F_s \tag{2}$$

$$F_p = F_s + F_o = \frac{l}{q} \cdot F_s \tag{3}$$

where k_s is the elastic constant of the internal springs. It follows that the output torque $\tau = F_o \cdot R$ is

$$\tau = \frac{l-q}{q} \cdot R \cdot k_s \cdot s = \left(\frac{l-q}{q} \cdot R\right)^2 \cdot k_s \tag{4}$$

and the output stiffness of the SAM

$$K = \frac{\partial \tau}{\partial \phi} = \left(\frac{l-q}{q} \cdot R\right)^2 \cdot k_s \tag{5}$$

which can indeed be adjusted by varying q, and scales linearly with k_s.

B. Torque-Deflection Workspace

A sufficiently large torque-deflection workspace is of central importance to the performance of a VSA. The actuator's ability to change its output stiffness, can only be exploited, if the VSA can exchange energy with the environment.

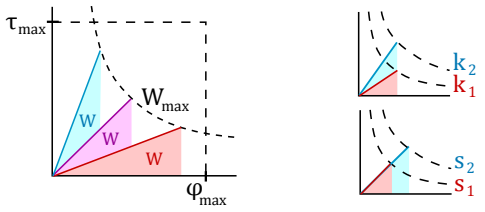

Fig. 3: The torque-deflection workspace of a lever-arm based VSA is limited by the maximum torque $\tau_{\max}$, deflection $\phi_{\max}$ and energy capacity of the internal springs $W_{\max}$, which is the area under the torque-deflection characteristic. $W_{\max}$ depends on the stiffness k and deflection s of the spring, as the energy stored in a spring is $\frac{1}{2}\, k\, s^2$. Increasing the stiffness k, linearly increases the output torque for a given deflection and stiffness setting, while increasing s allows the VSA to be deflected further, scaling the absorbed energy with s^2, as can be seen in the right part of the Figure.

The maximum energy that can be absorbed through the output, is the energy that the VSA can store in its internal spring element:

$$W_{\max} = \int_0^{\phi_{\max}} \tau(\phi)\, \mathrm{d}\phi = \frac{1}{2}\, k_s\, s_{\max}^2 \tag{6}$$

It is clear from Eq. 6 that the torque-deflection workspace can be increased by stiffer springs or a larger maximum spring deflection, i.e. a larger energy storage of the springs.

The workspace boundary can be expressed through pairs of τ and ϕ at the maximum spring deflection. The output deflection $\phi(q, s)$ as a function of the spring deflection s is obtained by reformulating Eq. 1:

$$\phi = \arcsin\left(\frac{q}{l-q} \cdot \frac{s}{R}\right) \tag{7}$$

while the output torque $\tau(q, s)$ is given in Eq. 4.

The connection between energy storage in the VSA and the spring parameters k_s and $s_{\max}$ is illustrated in Fig. 3, together with the influence of k_s and $s_{\max}$ on the VSA's torque-deflection workspace.

C. Internal Loads

It can be seen from Eq. 2 and 3, that the internal loads on the pivot point of the SAM do not only depend on the output force F_o and spring force F_s, but also on the transmission ratio between output and spring, defined by the pivot position q. The same output load might lead to undesirably large internal forces at unfavorable lever-arm ratios.

Eq. 7 can be rewritten to give the pivot position q for a given output and spring deflection

$$q = \frac{l}{1 + \frac{s}{R \cdot \sin(\phi)}} \tag{8}$$

The ratio of the pivot and output forces is

$$\frac{F_p}{F_o} = \frac{l}{l-q} = 1 + \frac{R \cdot \sin(\phi)}{s} \tag{9}$$

The higher this ratio is, the larger the internal forces acting in the mechanism become for a given load at the output.

Fig. 4 shows $\frac{F_p}{F_o}$ as a function of the maximum spring deflection s_{max} for several output deflections. It can be seen

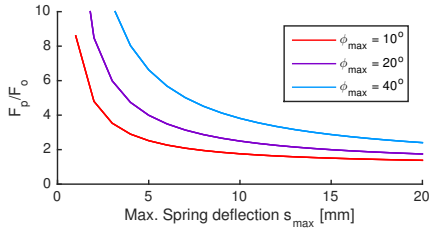

Fig. 4: The ratio of the forces at the pivot point and the output at maximal deflection and load as function of the maximum spring deflection for $R = 50$mm.

that the load on the pivot point becomes much larger compared to the force at the output, at small spring deflections. This is because a small spring deflection requires the pivot to be close to the springs, if a large output deflection is required, which leads to unfavorable lever arm ratios with respect to the internal loads.

D. Design Guidelines

The key design requirements for the springs for a lever arm based VSA have been identified to be:

- *Energy Storage Capacity:* Maximize the energy storage capacity of the springs to allow a large torque-deflection workspace and compliant interaction with the environment.
- *Internal Loads:* Limit the internal loads on the pivot for a given output load.
- *Compactness:* The springs need to fit inside the typically cylindrical enclosure of the VSA, without obstructing the motion of the lever.

We address these requirements by proposing the following guidelines for the design of the elastic elements:

- *Energy Storage:* The shape and material of the spring need to be chosen such that they maximize the energy storage capacity.
- *Maximum Spring Deflection:* Set a required maximum spring deflection $s_{\max}$, in this case 10mm, to limit the internal loads according to Eq. 9. This means that the spring's stiffness k needs to be maximized to achieve a maximum energy $E = k\,s^2$.
- *Utilize the Mounting Volume:* To ensure a compact design, an Ω-shaped leaf spring is chosen as elastic element. It exploits the available space better than the coil extension [7] [8] or torsion springs [9] that are mounted perpendicular to the lever in most other VSA of this type.

III. Design Methodology for Leaf Springs

The following section investigates how leaf springs can be layed out to maximize their energy storage capacity, given the design requirements imposed by the SAM. The equations are derived for straight beams, but the design guidelines and relationships between the spring's parameters still hold true for the Ω-shaped spring designed using Finite Element Analysis, as presented at the end of this section.

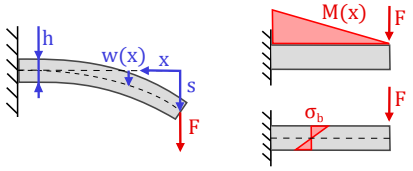

Fig. 5: A leaf spring with one fixed and one free end loaded by the force F, and the distribution of the resulting bending moment and stress.

A. Euler-Bernoulli Beam

Leaf springs can be modeled as an Euler-Bernoulli beam, assuming a slender beam with small deflections $w(x)$, where x denotes the distance from the spring's free end along its neutral fiber. For the simple case of a beam with constant, rectangular cross section with height b and thickness h, area moment of inertia $I = \frac{b\,h^3}{12}$, and constant flexural modulus E, with one fixed end, and that is loaded with the force F at its free end, as shown in Fig. 5, the maximal deflection occurs at the free end of the lever and is [11]

$$w(0) := s = \frac{F \cdot l^3}{3 \cdot E \cdot I} = \frac{4 \cdot F \cdot l^3}{E \cdot b \cdot h^3} \tag{10}$$

The stiffness of the spring is

$$k = \frac{dF}{ds} = \frac{3\,E\,I}{l^3} = \frac{E\,b\,h^3}{4\,l^3} \tag{11}$$

The maximum energy that can be stored in the spring now depends on the maximum spring deflection, achieved when the stress in the spring reaches its permissible limit. The maximum bending stress occurs at the surface of the fixed end of the beam, where the moment $M_b(l)$ is largest [11]

$$\sigma_{\max} = \frac{M_b(l)}{I}\,\frac{h}{2} = \frac{6\,F\,l}{b\,h^2} \tag{12}$$

leading to the load

$$F = \frac{\sigma_{\max}\,b\,h^2}{6\,l} \tag{13}$$

which, substituted into Eq. 10, gives the maximum deflection

$$s_{\max} = \frac{2}{3}\frac{l^2}{h}\frac{\sigma_{\max}}{E} \tag{14}$$

And thus the maximum energy that can be stored in the spring is

$$\begin{aligned} W_{b\,\max} &= \frac{1}{2}\,F\,s_{\max} = \frac{1}{2}\,k\,s_{\max}^2 \\ &= \frac{1}{2}\,\frac{E\,b\,h^3}{4\,l^3}\,\left(\frac{2}{3}\frac{l^2}{h}\frac{\sigma_{\max}}{E}\right)^2 \\ &= \frac{1}{9}\,\frac{\sigma_b^2}{2\,E_b}\,b\,h\,l = \eta_A\,\frac{\sigma_b^2}{2\,E_b}\,V \end{aligned} \tag{15}$$

with the degree of volume utilization $\eta_A = 1/9$, specific energy absorption capacity $\frac{\sigma_b^2}{2\,E_b}$ and volume $V = b\,h\,l$.

The degree of volume utilization η_A [12], or form coefficient C_F [11], accounts for a non-uniform stress distribution, comparing the actual energy stored in the material with the highest possible energy stored in the same volume.

B. Optimizing Spring Parameters

Eq. 15 shows, that the maximum energy capacity of a spring depends on three factors:

- the degree of volume utilization η_A,
- the specific energy storage capacity $\frac{\sigma_{\max}^2}{2\,E}$ of a material,
- the total volume V of the spring.

As shown above, a leaf spring with a constant cross section does not utilize its material very well for energy storage. This is because the bending moment is not constant along its length, as shown in Fig. 5, and the highest stress only occurs at the spring's fixed end, leading to the stress distribution

$$\sigma_{max}(x) = \frac{M(x)}{I(x)}\frac{h}{2} = \frac{6\,F\,x}{b(x)\,h(x)^2} \tag{16}$$

For a parabolic spring with variable thickness $h(x) = h_0\,\sqrt{x/l}$, or a triangular spring with variable height $b = b_0\,x$, however, the maximum stress is spread evenly over the lateral surface of the spring. The degree of volume utilization for such a spring of uniform strength is $\eta_A = \frac{1}{3}$ [12], three times larger than for a constant cross section. The energy storage capacity of a leaf spring can thus be much improved by choosing a favorable geometry, leaving the dependency on the material properties and spring volume to be investigated.

Usually the mounting dimensions only constrain b and l, while h is often not significant for the volume of the SAM. This is because leaf springs are slender structures, and their thickness is typically much smaller than their length.

For a given deflection $s_{\max}$, height b, and length l, the thickness h of the beam can be chosen, such that the bending stress σ does not exceed the permissible stress $\sigma_{\max}$, which gives the thickness of the beam from Eq. 14 as

$$h = \frac{2\,l^2\,\sigma_{\max}}{3\,E\,s_{\max}} \tag{17}$$

This represents a way to maximize the spring's volume and thus energy absorption, given constraints on l, b and s. The spring's volume $V = l \cdot b \cdot h$ is now also a function of its maximum deflection s and the material properties $\sigma_{\max}$ and E. Substituting Eq. 17 into Eq. 15, the maximum energy the spring can absorb becomes

$$W_b = \frac{1}{9}\,\frac{\sigma_{\max}^2}{2\,E}\,b\,h\,l = \frac{1}{27}\,\frac{b\,l^3}{s_{\max}}\,\frac{\sigma_{\max}^3}{E^2} \tag{18}$$

and substituting Eq. 17 into Eq. 11 its stiffness

$$k = \frac{2}{27}\,\frac{b\,l^3}{s_{\max}^3}\,\frac{\sigma_{\max}^3}{E^2} \tag{19}$$

Note that $\frac{\sigma_{\max}^3}{E^2}$ appears as a new factor, that is proportional to the spring's stiffness and energy absorption capacity, and is determined by the material properties given in Table I. The material properties are thus not only important for the specific energy storage capacity, but also for the additional constraint on a required spring deflection $s_{\max}$.

C. Spring Materials

The specific energy capacity $\frac{W}{V} = \frac{\sigma^2}{2\,E}$ is quadratic to the elastic limit of the material, and inversely proportional to its elastic modulus, meaning that though, i.e. strong and elastic, materials are required. As such, high strength spring steels, copper and nickel alloys are the most common spring materials [11], [13], but also plastics, mostly fibre-reinforced polymers, and rubbers are being used for special applications.

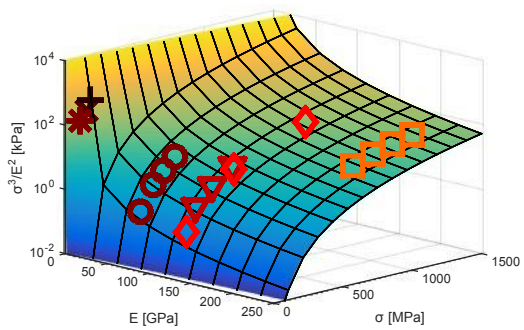

Fig. 6: The metric $\frac{\sigma^3}{E^2}$ for the energy absorption capacity of a leaf spring with given length l, height b and maximum deflection s. Due to their low flexural modulus, engineering plastics (POM: *, PET: X, PEI: +) outperform strong but rigid metals (aluminum: O, phosphor bronze: Δ, beryllium copper: ♢, steel: □).

For many materials the flexural strength is the same as the tensile or compressive strength. Especially for engineering plastics, however, the flexural strength may lie above the tensile strength, and is thus also given in Table I, together with the flexural modulus.

Table I shows the elastic modulus and permissible stress for a number of different spring materials, along with their specific energy storage capacity. Fig. 6 shows the metric $\frac{\sigma_{\max}^3}{E^2}$ as a function of the material's bending yield strength and flexural modulus. It can be seen that even though metals generally have a higher specific energy capacity $\frac{\sigma_{\max}^2}{2\,E}$ than plastics, engineering plastics can achieve a higher energy storage when considering $\frac{\sigma_{\max}^3}{E^2}$, which takes the special requirements of lever arm VSAs into account.

It must be noted that the values given in Table I may still vary considerably for a given material, and depend on many factors, such as the chemical composition, production process, or heat treatment. Likewise the list of materials is far from exhaustive. However, it shows values representative of the most common materials used for springs over a large range of strength and elasticity.

D. Finite Element Analysis

The design guidelines derived in this section were put into effect with a finite element analysis. The springs need to fit within the mounting volume, without obstructing the lever, and were laid out for a maximum deflection $s_{max} = 10mm$, as motivated in Section II-C.

In order to maximize the energy capacity, the springs were designed to be as stiff as possible by achieving an as uniform as possible stress distribution close to the permissible stress. This has been carried out in Ansys for two materials, spring steel and POM. Spring steel was chosen as a classical spring material with high strength, while POM represents flexible

TABLE I: Material Properties for Selected Spring Materials

Material	$\sigma_{n\,\text{yield}}$ [MPa]	E [GPa]	$\sigma_{b\,\text{yield}}$ [MPa]	E_b [GPa]	$\frac{\sigma^2_{b\,\text{yield}}}{2\,E_b}$ [MPa]	$\frac{\sigma_{b\,\text{yield}^3}}{E_b^2}$ [kPa]
Spring Steel (51CrV4) [13]	840 - 1260	206	840 - 1260	206	1.71 - 3.85	14.0 - 47.1
Beryllium Copper (CuBe2) [13]	140 - 1000	122	140 - 1000	122	0.080 - 4.01	0.184 - 67.2
Phosphor Bronze (CuSn6) [13]	230 - 500	118	230 - 500	118	0.224 - 1.06	0.874 - 8.98
Aluminum (ENAW-2014) [13]	125 - 380	70	125 - 380	70	0.112 - 1.03	0.399 - 11.2
POM-C (Tecaform AH) [14]	67	2.8	91	2.6	1.59	111
PET (Tecadur PET) [14]	91	3.3	134	3.4	2.64	208
PEI (Tecapei) [14]	127	3.2	164	3.3	4.08	405

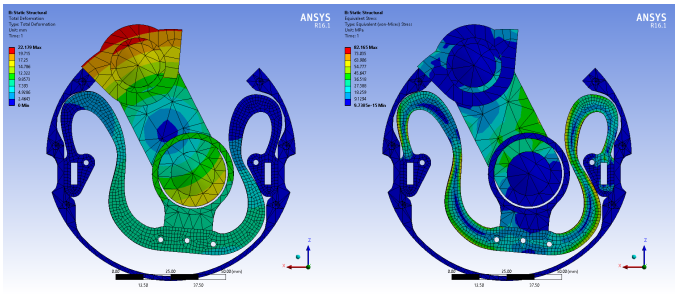

Fig. 7: Results of the Finite Elements Analysis showing the total deflection and von-Mises stress for the POM spring at full deflection.

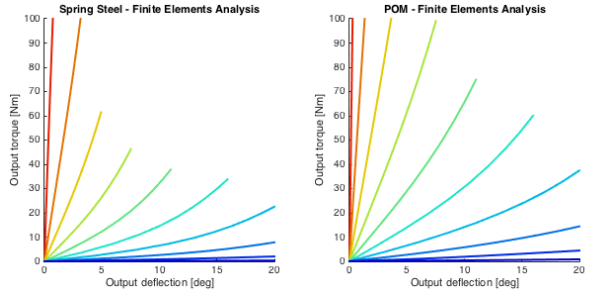

(a) (b)

Fig. 8: Simulated torque-deflection workspace for a steel and POM spring.

polymers that are increasingly utilized as spring elements, with 210 GPa and 2.6 GPa as flexural moduli and 950 MPa and 90 MPa as flexural yield strengths.

The stress in the spring was verified for a range of pivot positions of the lever, as the precise stress distribution and motion of the spring depend on the internal transmission. Fig. 7 shows the deformation and stress of the POM spring at maximum spring and output deflection.

Fig. 8 shows the simulated torque-deflection workspace of the springs. It can be seen that the POM spring achieves a larger workspace than the steel spring; the more flexible POM could be made much thicker and thus stiffer than steel, while still reaching the same maximum deflection, as predicted by the metric $\frac{\sigma^3}{E^2}$.

IV. Experiments

In order to verify the results of the FEA, the lever arm based VSM, shown in Fig. 1, was equipped with both a spring made from spring steel and POM, that were manufactured from stacked layers that were laser-cut from 3mm thick sheet material. A section view showing the structure of the VSM, that is based on the design of [7], is given in Fig. 9. The lever-arm mechanism with leaf spring and pivot bearing can be seen at the top of the SAM. Below it, a hypocyclic gear mechanism moves the pivot point in a straight line. The mechanism is actuated through a RoboDrive motor and Harmonic Drive strain wave gear.

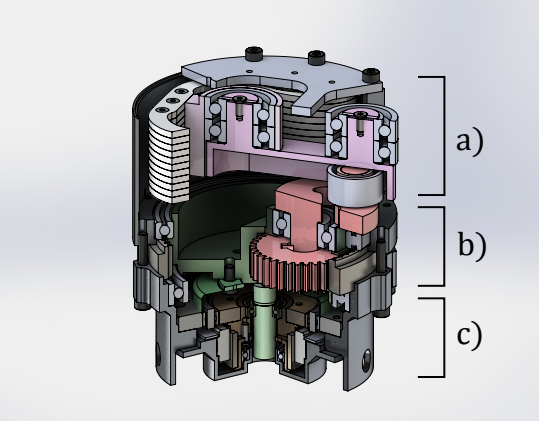

Fig. 9: Cross-section of the VSM used for the experiments. The lever-arm mechanism a), planetary gear mechanism b), and actuation c) can be seen.

The torque-deflection characteristics, shown in Fig. 10, were recorded by manually deflecting the output of the VSM via a lever carrying a Schunk FT-Mini-40 force sensor, while measuring the output deflection with an integrated ams AS5047P absolute magnetic rotary encoder. The stiffness was adjusted between the measurements by changing the actuated pivot position of the VSM in 5mm increments along the length of the lever.

As predicted by the analysis and simulations in Section III, the POM spring is stiffer and achieves a larger torque deflection workspace than the stel spring, though also shows more hysteresis, which is negligible for the steel spring. Both springs show an increased hysteresis in the third quadrant, which is likely caused by friction in the VSM setup. The play of ca. 2° visible in the measurements is mostly caused by backlash in the actuation of the pivot.

The workspace limit, defined by the spring's end-stops, are shown in Fig. 10 where calculated with the passive output deflection from Eq. 7 at maximum spring deflection

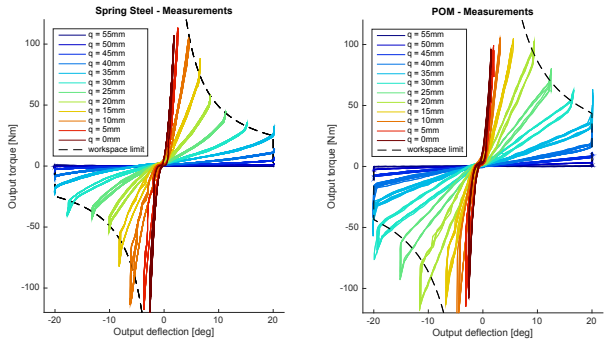

(a) (b)

Fig. 10: Torque-deflection measurements of the VSM equipped with a POM and Steel spring.

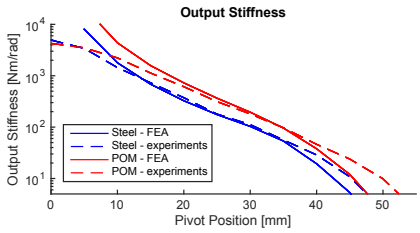

Fig. 11: Semi-logarithmic graph of the simulated and measured output stiffness for a steel and POM spring as function of the pivot position.

$s_{max} = 10$mm and the corresponding output torque from Eq. 4. The spring stiffness has been set to match the experimental results, and was found to be approximately 0.085N/mm and 0.15N/mm for the steel and POM springs respectively.

The simulated and measured output stiffness is shown in the semi-logarithmic graph in Fig. 11, and shows a good accordance between measurements and FEA simulations. Only for pivot positions below 15mm the parasitic compliance of the VSM becomes apparent, when the measured output stiffness for both springs approaches 5000 Nm/rad in stead of infinity. Likewise, for pivot positions above 35mm the experimental stiffness values approach zero slower than in the simulations.

V. DISCUSSION

Both the simulations and experiments confirm that a flexible polymer spring can achieve greater stiffness, and thus energy storage, than a strong metal spring, when they are laid out for the same spring deflection. This makes engineering plastics very suited as elastic elements in physically compliant robotic applications, which themselves are a growing field. Especially when considering the spread of rapid prototyping technologies, that drastically increases the ease of manufacturing of custom made polymer springs.

Metal springs, on the other hand, are a proven material that exhibit other advantages over polymers, such as lower damping and hysteresis, much higher resistance to creep, and a larger operating temperature range. However, when selecting a material for a spring element, its properties, manufacturing process, availability and cost all need to be taken into account. Engineering Polymers offer an interesting option, where other high performance polymers, or fiber-reinforced materials, can often outperform POM, which was used in this comparison.

It has furthermore been shown here, that a suited method for designing an elastic element, can also drastically increase the springs performance, and a proper analysis is crucial for a high performance solution.

VI. CONCLUSIONS

This paper presented a method for the design of the internal elastic elements of a lever-arm-based VSA, that maximize the energy storage of the actuator, while keeping the design compact and accounting for characteristics of this sub-class of VSA.

It was shown that the theoretical analysis carried out, in combination with a FEA, can lead to a design that maximizes the VSA's torque-deflection workspace and energy storage capacity. Finally, the results were verified through experiments with a VSA equipped with steel and polymer springs.

REFERENCES

[1] B. Vanderborght *et al.*, "Variable impedance actuators: Moving the robots of tomorrow," in *Proceedings of the IEEE/RSJ International Conference on Intelligent Robots and Systems*, 2012, pp. 5454–5455.

[2] R. Pfeifer and J. Bongard, *How the body shapes the way we think: a new view of intelligence*. MIT press, 2006.

[3] G. Grioli *et al.*, "Variable impedance actuators: The user's point of view," *International Journal of Robotic Research*, vol. 34, no. 6, pp. 727–743, 2015.

[4] B. Vanderborght *et al.*, "Variable impedance actuators: A review," *Robotics and Autonomous Systems*, vol. 61, no. 12, pp. 1601–1614, 2013.

[5] S. Wolf, O. Eiberger, and G. Hirzinger, "The DLR FSJ: Energy based design of a variable stiffness joint," in *Proceedings of the IEEE International Conference on Robotics and Automation*, 2011, pp. 5082–5089.

[6] R. V. Ham, B. Vanderborght, M. V. Damme, B. Verrelst, and D. Lefeber, "MACCEPA, the mechanically adjustable compliance and controllable equilibrium position actuator: Design and implementation in a biped robot," *Robotics and Autonomous Systems*, vol. 55, no. 10, pp. 761 – 768, 2007.

[7] S. Groothuis, G. Rusticelli, A. Zucchelli, S. Stramigioli, and R. Carloni, "The vsaUT-II: a novel rotational variable stiffness actuator," in *Proceedings of the IEEE International Conference on Robotics and Automation*, 2012, pp. 3355–3360.

[8] N. Tsagarakis, I. Sardellitti, and D. Caldwell, "A new variable stiffness actuator (CompAct-VSA): Design and modelling," in *Proceedings of the IEEE/RSJ International Conference on Intelligent Robots and Systems*, 2011, pp. 378–383.

[9] A. Jafari, N. Tsagarakis, and D. Caldwell, "AwAS-II: A new actuator with adjustable stiffness based on the novel principle of adaptable pivot point and variable lever ratio," in *Proceedings of the IEEE International Conference on Robotics and Automation*, 2011, pp. 4638–4643.

[10] L. C. Visser, R. Carloni, and S. Stramigioli, "Energy-efficient variable stiffness actuators," *IEEE Transactions on Robotics*, vol. 27, no. 5, pp. 865–875, 2011.

[11] J. Collins, H. Busby, and G. Staab, *Mechanical Design of Machine Elements and Machines*. Wiley, 2010.

[12] J. Grote, K.-H. and. Feldhusen, *Dubbel*. Springer Berlin Heidelberg, 2007.

[13] H. Wittel, H. Roloff, and W. Matek, *Roloff/Matek Maschinenelemente: Tabellenbuch*, ser. Viewegs Fachbücher der Technik. Vieweg & Teubner, 2009.

[14] Ensinger GmbH, http://www.ensinger-online.com/en/materials/.